Original Article

# Colorectal cancer mouse metastasis model combining bioluminescent and micro-computed tomography imaging for monitoring the effects of 5-fluorouracil treatment

**Wei-Jie Song[1,2,3], Fan Zhang[1,2,3], Zhi-Yong Wang[1,2,3], Zhao-Song Wang[1,2,3], Bi-Yun Wang[1,2,3], Jun-Rong Jia[1,2,3]**

[1]Laboratory Animal Center, Tianjin Medical University Cancer Institute and Hospital, National Clinical Research Center for Cancer, Tianjin, China; [2]Tianjin's Clinical Research Center for Cancer, Tianjin, China; [3]Key Laboratory of Cancer Prevention and Therapy, Tianjin, China

*Contributions:* (I) Conception and design: WJ Song, F Zhang; (II) Administrative support: ZY Wang, ZS Wang; (III) Provision of study materials or patients: BY Wang, JR Jia; (IV) Collection and assembly of data: WJ Song, F Zhang; (V) Data analysis and interpretation: WJ Song, ZY Wang, ZS Wang; (VI) Manuscript writing: All authors; (VII) Final approval of manuscript: All authors.

*Correspondence to:* Wei-Jie Song, MD. Laboratory Animal Center, Tianjin Medical University Cancer Institute and Hospital, National Clinical Research Center for Cancer, Huan-Hu Western Road, Tianjin 300060, China; Tianjin's Clinical Research Center for Cancer, Tianjin 300060, China; Key Laboratory of Cancer Prevention and Therapy, Tianjin 300060, China. Email: wsong@tmu.edu.cn.

**Background:** Colorectal cancer (CRC) is the fifth most fatal cancer with a low probability of surgery and limited treatment options, especially in metastatic CRC. In this study, we investigated whether a mouse model of metastatic CRC mimicked tumor progression and evaluated the effect of 5-fluorouracil (5-FU) treatment.

**Methods:** The CT26 mouse derived CRC cancer cell line was inoculated into mice, and the tumor bearing mice were divided into two groups: the experimental group and the control group. Micro-computed tomography (CT) and *in vivo* fluorescence were used to monitor the progression of metastatic CRC. A lung metastasis mouse model was employed to determine the effects of 5-FU on metastasis.

**Results:** Bioluminescence imaging (BLI) and computed tomography (CT), as non-invasive methods, can continuously monitor the growth of tumors *in vivo*. Thus, imaging techniques can be used to qualitatively and quantitatively evaluate tumor growth indicators. 5-FU injected intravenously reduced the viability of metastatic CRC cells and resulted in prolonged survival compared to the control group. Moreover, the 5-FU-treated group had significantly reduced fluorescence of the CT26 cells in the lung. The results observed by BLI and CT are consistent with the tissue morphology and structure presented in pathological examination.

**Conclusions:** In summary, a successful mouse model of CRC metastasis for clinical application has been established.

**Keywords:** Mouse model; colorectal cancer (CRC); bioluminescent; micro-computed tomography (micro-CT); 5-fluorouracil (5-FU)

Submitted Mar 25, 2023. Accepted for publication Sep 21, 2023. Published online Oct 19, 2023.
doi: 10.21037/tcr-23-522
**View this article at:** https://dx.doi.org/10.21037/tcr-23-522

## Introduction

Colorectal cancer (CRC) is one of the most commonly diagnosed cancers, with increasing prevalence in different populations and a high mortality rate (1,2). The overall 5-year survival rate of CRC patients is 65%. However, when CRC metastasizes to distant organs, the 5-year survival rate falls to <20% (3). Most CRC patients die from metastases [metastatic CRCs (mCRCs)], particularly those found in the liver, lungs, and lymph nodes (4). The primary therapeutic approach for mCRC is surgical removal of metastases

with or without chemotherapy. mCRCs are not effectively treated with current therapeutic options. In recent decades, although the development of fluoropyrimidine-based [5-fluorouracil (5-FU), capecitabine] regimens FOLFOX (5-FU, leucovorin, oxaliplatin) and FOLFIRI (5-FU, leucovorin, irinotecan) has improved prognosis of patients, disease recurrence is still unstoppable. 5-FU has been used for years, and it remains the first-line drug used in CRC chemotherapy (5). However, more effective therapies are needed to improve the survival rate of CRC patients, especially patients with advanced disease stages.

The mouse model is crucial for understanding the biological, cellular, and molecular mechanisms underlying the occurrence and development of CRC, as well as evaluating the efficacy of treatment regimens. Xenograft models have been established to study human CRC cellular targets by subcutaneous (SC) or orthotopic implantation into the colon and rectal wall and by inoculation of human CRC cell lines into immunocompromised mice (6-9). Orthotopic xenograft models provide a more suitable environment for CRC cells to acquire malignant features than SC models, but they are more difficult to use (10). In contrast, due to the convince of cancer cell vaccination and tumor volume monitoring by direct measurements, SC tumor xenografts have been widely used (11). In addition, tumor volume is positively correlated with tumor weight. However, sequential monitoring of CRC growth or metastasis to remote area is more challenging with a short period of study (12,13). Thus, there is a need for a more biologically relevant mouse model to test treatment strategies and monitor the progression of metastasis in advanced-stage CRC. Preclinical models of CRC are critical for the development of new treatment strategies; however, only a few preclinical CRC mouse models are available. There are also genetically engineered models (14,15). Researchers face increasing difficulty in selecting animal models due to differing results among laboratories. In addition, treatment regimens that show promising results in SC heterotopic mouse models typically have little impact on cancer patients in clinical settings (10,16).

Due to its extremely targeting performance, high sensitivity, and low background pollution, *in vivo* bioluminescence imaging (BLI) technology has been widely used in cancer research (17-19). Bioluminescence is the ability of organisms to produce light, which is widely observed in fireflies, fungi, beetles, bacteria, and marine organisms. BLI involves the natural conversion of chemical energy into light or photons by using enzymes called luciferases or photoproteins and binding them to substrates called luciferins (20). It can be used to evaluate tumor growth, invasion and metastases by measuring the intensity of bioluminescence in animal models. The metastasis mouse model is considered to simulate natural tumor development in humans, as primary tumors have similar tumor microenvironment (21). We found that the CT-26-WT-LUC cell line, which was constructed from a liver metastasis in a CRC mouse, could cause metastatic lung tumors in mice, and we successfully formed a tumor through SC injection. This indicates that the mouse lung is a suitable microenvironment to supply the development of CRC tumors (22).

The objective of this study was to establish a model of CRC lung metastasis in nude mice using luciferase-marked CRC cell lines (CT26) to observe the progress of metastasis in the mouse models and assess the effects of 5-FU treatment in a clinically relevant tumor metastasis model. We present this article in accordance with the ARRIVE reporting checklist (available at https://tcr.amegroups.com/article/view/10.21037/tcr-23-522/rc).

**Highlight box**

**Key findings**

- A mouse colorectal cancer (CRC) model of lung metastasis was monitored with *in vivo* imaging and micro-computed tomography (CT) to investigate the therapeutic effect of 5-fluorouracil (5-FU).

**What is known and what is new?**

- Metastasis of CRC to distant organs is a common cause of death in patients.
- By far, there are no effective therapeutic drugs and clinical treatment for patients with CRC metastasis. We therefore focus on creating suitable disease models for more precise treatment.

**What is the implication, and what should change now?**

- This study highlights the important role of the CRC mouse model of lung metastasis in drug therapy and clinical treatment. Our findings combined with auxiliary examination methods such as *in vivo* imaging and micro-CT provide a direction for selecting a more effective treatment.

## Methods

### *Animals and experimental design*

Twenty BALB/c nude mice (Beijing Vital River Laboratory Animal Technology Co., Ltd., Beijing, China) aged 4–5 weeks old were injected intravenously (i.v.) with $5.0\times10^5$ CT26 cells. The mice were randomly divided into

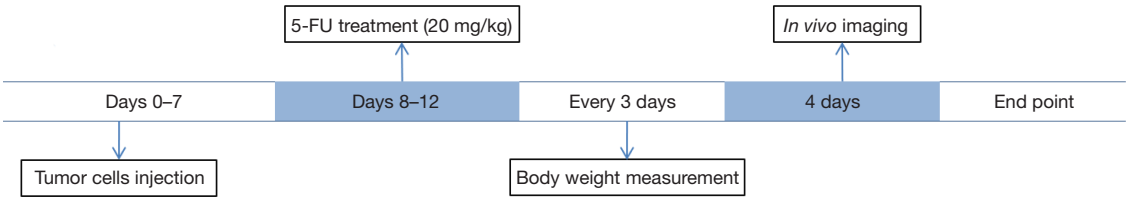


**Figure 1** Schematic showing the process of CT26 cell injection, body weight monitoring and *in vivo* imaging. Tumor cells were inoculated within a week, and then 5-FU solution was injected into the abdominal cavity on days 8 to 12. Mouse body weight was monitored every 3 days, and tumor growth was monitored 4 days after monitoring weight with a frequency of once a week through bioluminescence imaging until the end point. 5-FU, 5-fluorouracil.

two groups 7 days after tumor injection. On days 8 to 12, the mice were injected intraperitoneally (i.p.) with 5-FU (20 mg/kg). The doses of 5-FU were adapted and modified from a previous study (23). BLI was applied to monitor intrapulmonary tumor growth with luciferase-expressing tumors (*Figure 1*). The animals were housed in individual ventilated cages (Shinva Medical Instrument Co., Ltd., Zibo, China). In the experimental period, animals were kept in a limited access, air-conditioned room (room temperature: 20–26 ℃, relative humidity: 40–46%, 10–15 air changes/h, 12 h light cycle). Food and water were available *ad libitum* (food: Jiangsu Xietong Pharmaceutical Bio-engineering Co., Ltd., Nanjing, China). All experiments were conducted according to local institutional guidelines for the care and use of animals and approved by the Animal Care and Use Committee of Tianjin Medical University Cancer Institute & Hospital, Tianjin, China (Animal Protocol No. 2022035).

### *Main reagents*

Phosphate-buffered saline (PBS) was purchased from Gibco company (Carlsbad, CA, USA). Dulbecco's modified Eagle's media (DMEM) and RPMI-1640 were purchased from HyClone Company (HyClone, Logan, UT, USA). Fetal bovine serum (FBS), streptomycin and penicillin were purchased from Gibco (Carlsbad, CA, USA). Firefly luciferase-lentiviruses and Polybrene were ordered from GENECHEM (Promega, WI, USA). D-Luciferin potassium salt was purchased from PROMEGA (Madison, WI, USA). Puromycin was purchased from Sigma-Aldrich (St. Louis, MO, USA). Medical anastomosis glue was obtained from Bai Yun Mountain Pharmaceutical Company (Guangzhou, China).

### *Cell cultures and experimental design*

The CT26 mouse cancer cell line was purchased from the American Type Culture Collection (ATCC) (Manassas, VA, USA). The cells were cultured in RPMI-1640 medium supplemented with 10% FBS and 250 mg/mL Geneticin (Thermo Fisher Scientific, MA, USA) at 37 ℃ and 5% $CO_2$. The medium was changed every third day. *In vivo* bioluminescence using Xenogen's IVIS imaging system (Caliper, PerkinElmer, Florida, USA) was performed as previously described (24).

### *Xenograft models*

A total of $5\times10^5$ luciferase-expressing CT26 tumor cells were injected into the caudal vein of 10 animals to create the intravenous xenograft model. The mice were secured with a special device to fully expose their tails. After wiping the tail with a cotton ball soaked in alcohol, the root of the tail was gently pinched and flicked at the injection site to fill and expand the blood vessels, or it was soaked in warm water at 45–50 ℃ for 30 seconds. Then, the tail was fixed with a thumb and index finger. The syringe was held in the right hand parallel to the vein and injected at 1/4 of the back of the mouse tail. The needle was pushed at least 3 mm easily without resistance. After injection, the site was pressed with a dry cotton ball, or the tail was bent in the direction of the injection to stop bleeding. If a repeated injection was needed, the technician started from the end of the tail and gradually moved toward the root of the tail.

### *BLI measures tumor growth and lung metastases*

All the cells were monitored using an IVIS Xenogen imaging system 1 week after injection, and then the mouse was observed once a week. Mice received an intraperitoneal injection of 150 mg/kg D-luciferin potassium salt solution according to the manufacturer's instructions. Imaging times ranged from 1 to 30 s, relying on the tumor growth and

 

time point. Generally, four to five mice were imaged at the same time in the field of view D.

Animals were anesthetized with 2.5% isoflurane. Image acquisition was performed 10 minutes after luciferin injection. Living Image software (Caliper) was used to measure the luciferase activity. Tumor-growing animals were sacrificed once the luminescence efficiency reached $5\times10^9$ photons (25). The mice exhibited signs of systemic or body weight decline 4 weeks after transplantation.

### *Pathology analyses*

Dissect the lung, liver, spleen, colon, stomach, and heart, then fix them in 10% phosphate buffered formalin, process and then embed them in paraffin (26). The embedded organs were cut into 5 $mm^3$ sections and stained with hematoxylin and eosin (H&E) and Alcian blue to display goblet cells. Observe the height of the villus under an optical microscope (Olympus Bx43, Tokyo, Japan) at a magnification of 10×, and measure the height from the base to the tip of the villus using an image analysis program (Olympus CellSense Dimension). To evaluate the effects of 5-FU on lung secretion, tumor cells were counted with ImageJ software. Stained slides were analyzed by light microscopy.

### *Statistical analysis*

The data collected from *in vitro* and *in vivo* experiments were statistically analyzed using GraphPad Prism 8 software. One-way ANOVA and *t*-tests were performed. The quantified bioluminescence intensity of the tumors was reported as the mean ± standard deviation. $P<0.05$ was considered to be statistically significant.

## Results

Each group of mice (n=10) was injected with CT26 cells based on imaging and Pathology data, as described below.

### *Tumor growth measurement*

BLI and micro-computed tomography (micro-CT) were used to monitor tumor growth longitudinally and noninvasively. Qualitative and quantitative indices of tumor growth were assessed. Living imaging has extremely high sensitivity, allowing for the detection of small tumor lesions (as few as one hundred cells), greatly improving the sensitivity compared to traditional methods. BLI values and tumor metastases were quantified at a predetermined time point and showed steady growth (*Figure 2A*). BLI was more suitable than micro-CT for identifying tumor development due to its higher sensitivity and reliability (*Figure 2B*). *Figure 2C* shows micro-CT and BLI images from a representative tumor-bearing animal from the CT26 cell line in the control group. In the CRC (CT26) cell line, tumor development was successfully monitored by BLI, while the corresponding micro-CT images did not detect the same extent of tumor development.

### *Tumor growth monitoring and 5-FU injection*

BLI involves the natural transformation of chemical energy into light, or photons, by using enzymes known as luciferases or photoproteins and coupling them with their substrates known as luciferins. Due to improvements in emission, the latest developments in BLI have enabled the visualization of individual tumor cells to increase from 100 to 1,000 times compared to traditional technologies (27). The mice receiving intravenous injection (i.v.) were randomly divided into two groups, and lung metastases were found 2 weeks after injection. At least 60% (3 of 5 mice versus 5 of 5 mice) of mice in both groups demonstrated lung metastases with enhanced BLI signals over time (*Figure 3A-3D*). There was a significant difference in fluorescence intensity between the groups receiving 5-FU and the control group (*Figure 3E*), the latter of which had higher fluorescence intensity 14 days after 5-FU injection (*Figure 3E*). Furthermore, only one mouse within the 5-FU-treated group survived by the last week (*Figure 3F*). Three weeks after CT26 cell injection, metastasis was observed by micro-CT (*Figure 3G*, where the green arrow indicates metastasis). As detected by weekly monitoring, there was a significant reduction in fluorescence intensity in the 5-FU group compared with the control group (*Figure 3E*).

### *5-FU treatment response*

For the CT26 model, fluorescence values of BLI based on tumor cells were measured as the corresponding logarithmic bioluminescence value at each time point (*Figure 3E*). Significant correlation between optical imaging values and tumors (Pearson correlation, $r=0.93$, $P=0.0001$) niche was detected for CT26 tumors (*Figure 3H*). To determine the ability of 5-FU to inhibit tumor growth in major metastatic sites, we performed

 

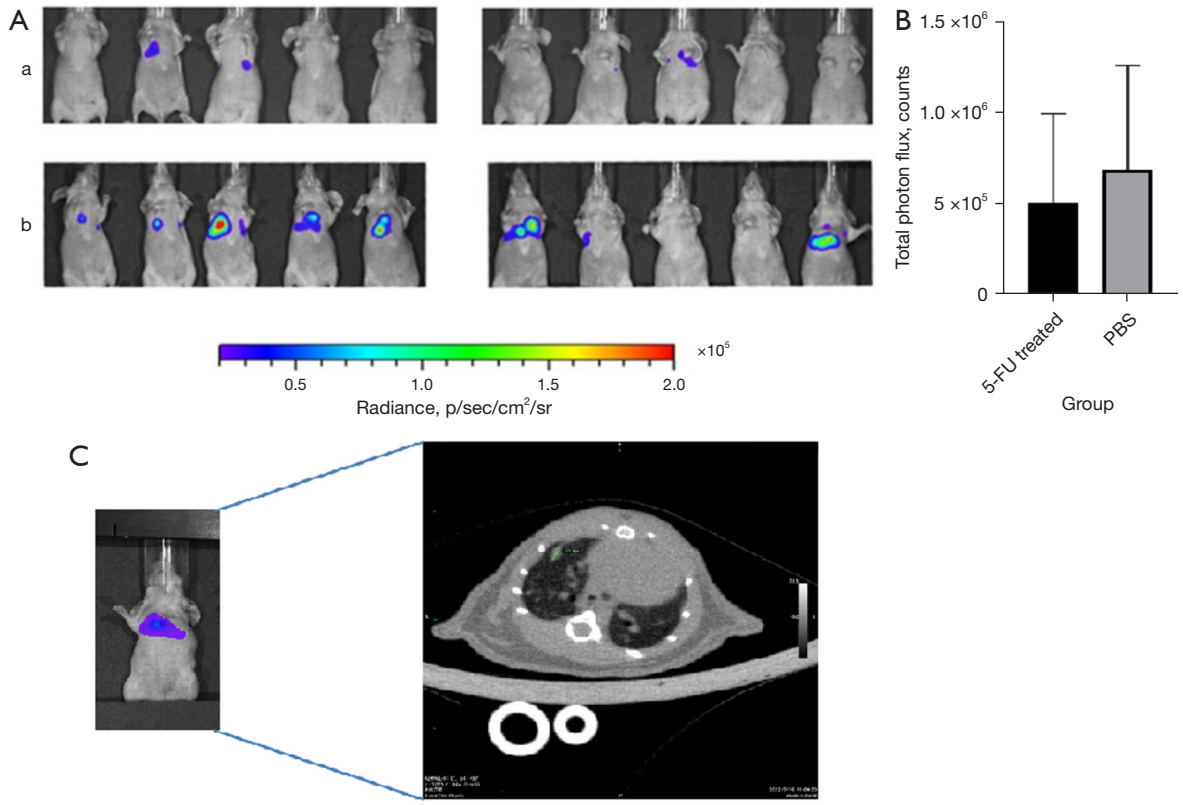


**Figure 2** Regular monitoring of the growth of tumor cells in tumor-bearing mice through BLI equipment and micro-CT scans. Nude mice were randomly divided into two groups and monitored *in vivo* using BLI and micro-CT (A,C). Group (a) was treated with 5-FU, and group (b) was treated with PBS as a control (A,B). Total photon flux was detected by bioluminescent in both groups (B). p, photon; sec, second; sr, steradian; PBS, phosphate-buffered saline; BLI, bioluminescence imaging; 5-FU, 5-fluorouracil; CT, computed tomography.

*in vivo* imaging of the lung of mice with CT-26 luciferase-expressing tumors. We confirmed that 100% of CT-26 luciferase-expressing tumors formed lung metastases follow i.v. injection (14). Using this spontaneous metastasis preclinical model, we determined that the 5-FU-treated mice had fewer lung metastases, suggesting suppression of tumors by 5-FU (*Figure 4A*). In a mouse with extensive lung metastases from the i.v. tail injection, daily i.p. 5-FU treatment for 5 days resulted in tumor suppression without recurrence after 1 month (*Figure 4B*). 5-FU treatment also induced complete suppression of cranial metastases from i.v. tail injection xenografts in 2 mice (*Figure 3E*).

### *Pathology characteristics*

Pathological examination showed the mode of lung metastasis formation.

CT26 tumor cells spread primarily within the chest spaces of the mice, followed by early metastases appearing within the lung (*Figure 4C,4D*). All tumor-bearing mice developed lung metastases following the injection. *Figure 3B* shows the proliferation indices of the different tumor models. Pathological observation showed that the tissue cells were arranged in a nest-like or clustered cord-like manner, with local necrotic foci visible. Cancer cells varied in size and morphology, with large and deeply stained nuclei and visible mitotic figures. The nucleoli were clear and consistent with the characteristics of CRC tissue. Tumor growth varied between groups (*Figure 4A*). These findings corresponded with the progression of the respective tumors.

## Discussion

CRC mouse models can be mainly divided into three types: (I) orthotopic transplant tumor models; (II) chemical induction models; and (III) metastasis models. Orthotopic CRC xenografts have been researched over the past two decades. These models are considered to successfully

 

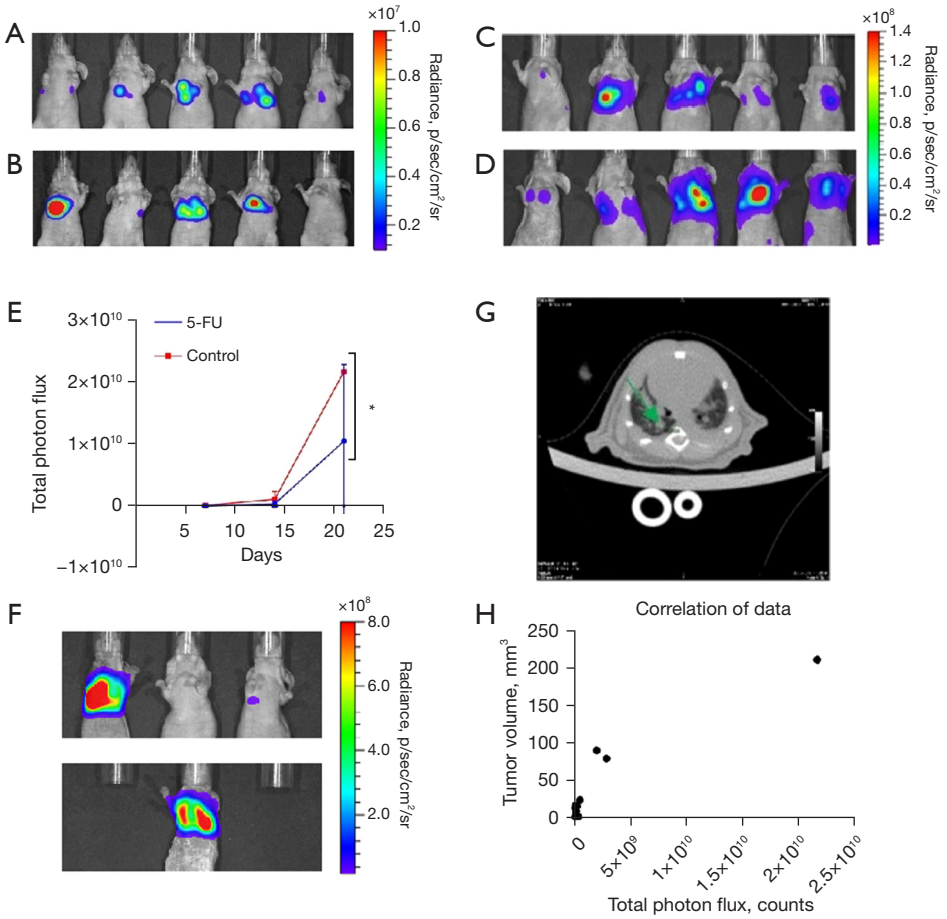


**Figure 3** Detection of tumor metastasis in mice by bioluminescence imaging and micro-CT. Tumor growth in the lungs was monitored during the first (A,B) and second (C,D) after mice were treated with 5-FU (A,C) or phosphate-buffered saline (B,D). Total photon flux was detected by bioluminescent and measured using the ROI. There was a significant difference between the 5-FU group and the control group (E). Mice were treated after 3 weeks with 5-FU (F) and observed by micro-CT. The position indicated by the green arrow is the lesion observed by CT (G). *In vivo* imaging results show a positive correlation between tumor photon count and lesion size (H). *, P<0.05. 5-FU group: n=10; control group: n=10. p, photon; sec, second; sr, steradian; 5-FU, 5-fluorouracil; CT, computed tomography; ROI, region of interest.

mimic lesion development and the microenvironmental characteristics of tumors in humans. They also allow for the evaluation of new therapies for tumor suppression in specific tissues related to clinical conditions. Many transplant techniques have been tested, including intrabronchial injection or intrapleural implantation of lung parenchyma after skin incision or surgical exploration of the pleura (28-31). The most suitable transplantation techniques and reliable models without major transplantation complications have yet to be established. The induced mouse tumor model refers to an experimental mouse tumor model induced by chemical carcinogens. Its drawbacks are long induction time, high animal mortality rate, and uneven phenotypes among individuals in terms of tumor appearance time, location, and number of lesions.

In this study, we established a mouse model of CRC lung metastasis using i.v. injection of CT26 cancer cells into nude mice. Immunodeficient mouse strains are insufficient for investigating the role of the immune system in tumor growth and therapeutic response. A genetically engineered mouse model with an intact immune system could be used to overcome this limitation for translational research. However, tumor development would take a long time using this model, and it would be difficult to investigate metastases due to uncertainties surrounding the site of the primary tumor, which would also reduce the killing of mice (32,33). Although

 

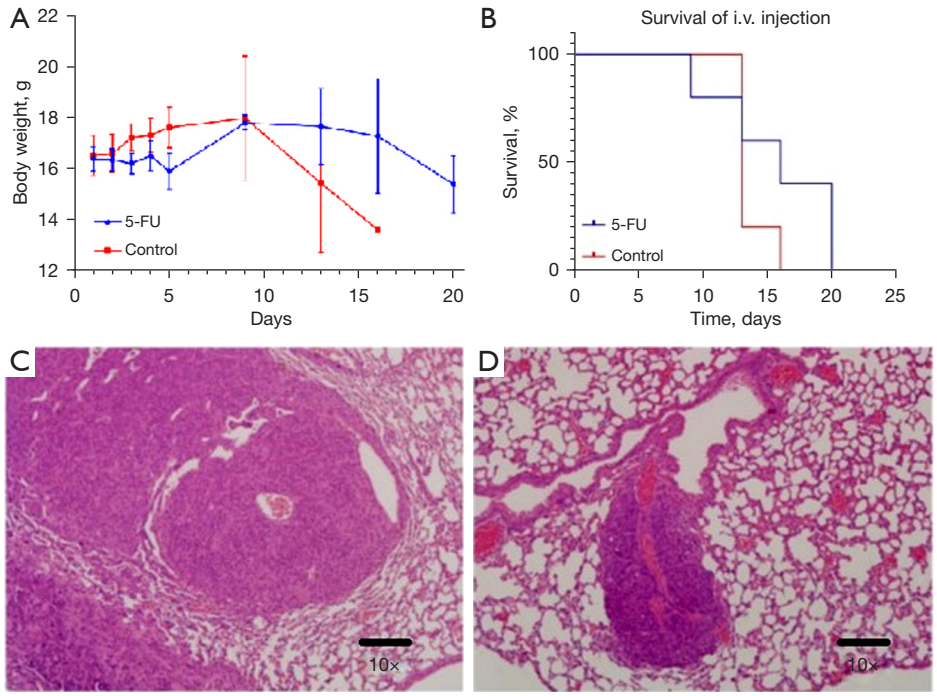


**Figure 4** The body weight of mice decreased in the first week following injection of 5-FU. After injecting 5-FU, body weight was monitored over the next 2 weeks (A). The survival curve displays the survival of mice during the 5-FU injection period (B). Pathological examination was completed for the control (C) and 5-FU (D) groups using a 10× microscope. Slices stained with hematoxylin-eosin method. 5-FU, 5-fluorouracil; i.v., intravenous.

it seems that injecting tumor cells into the mucosal surface via the cecum could mimic the CRC growth and dissemination observed in humans, achieving this would be technically challenging, and it would pose the risk of tumor cell leakage or spillage into the lumen (34-36). Instead, we established a lung metastasis model by delivering CT26 cancer cells i.v.

We also investigated the histological features of lung metastasis tumors as well as the survival curve to understand the growth pattern. Previous studies used a relatively large number of cells in a large volume suspension, which was associated with early metastasis to the lung. Therefore, these models often did not present with a primary lung tumor, which is necessary for testing the response to therapy (37,38). The model initially showed lesions (*Figure 2A*), which grew within an appropriate time before metastatic spread, allowing the provision of treatment within the desired window of time. The injection technique was simple and did not require any complicated technology. Along with the already published data, we dramatically decreased the number of CT26 cells in a small cell volume (500,000 cells in 50–100 µL) using a simple injection system, which requires a skilled operator of the injection (39). This technique starts with a localized lesion metastasized from the lung (*Figure 2A*,*2B*) 1 week after transplantation, mimicking the pathological development of CRC from primary lesions to metastatic disease.

We used micro-CT imaging for accurate measurement of tumor development. BLI and micro-CT were successfully applied to detect tumor growth. As previously observed in preclinical lung cancer models, we determined a significant correlation between signal intensity obtained by BLI and tumor volume (*Figure 2*), demonstrating the sensitivity and reliability of BLI in this model. The positive imaging and pathology data for the CT26 cell line were promising (100% mouse tumor model established). We found greater sensitivity using BLI and more reliability using micro-CT in C57BL/6N mice (40). It is possible that during the early tumor stage, intravenous growth at the injection site was not captured by micro-CT due to the transport of tumor cells into circulation. Therefore, BLI is more suitable for the detection of metastatic lung tumors as well as in circumstances when micro-CT values are uncertain. When evaluating tumor growth and particularly when locating tumors in uncharacterized models, the use of both

 

modalities together is recommended.

Considerations for the establishment of an experimental animal tumor model include the inoculation site of tumor cells, the number of inoculated cells and the choice of the experimental animals. There are various forms of tumor metastasis models, which are mainly divided into two categories: spontaneous metastasis models, which entail SC and *in situ* inoculation, and experimental metastasis models, which entail circulatory inoculation. The SC inoculation metastasis model has been used by scholars all over the world. However, establishing this model is expensive, and it is challenging to develop metastatic tumors and achieve the experimental requirements because the process is time-consuming. Tumors often break when there is no metastasis, and mice with excessive load develop cachexia. The CRC cancer metastasis model using orthotopic transplantation has become popular. Scholars believe that this model can accurately simulate the process of clinical metastasis. However, orthotopic transplantation is a difficult procedure because the mice are too small to handle. The operation must be performed in a sterile environment because nude mice are immune-deficient and prone to postoperative infection, resulting in a high risk of mortality. Our pathology data demonstrated the coordination of our imaging data in all models. The proliferation index demonstrated considerable differences between the two groups (*Figure 3D,3E*), which is similar to what is observed in a clinical setting (41).

## Conclusions

We established a metastatic CRC model that exhibits similar tumor growth to that seen clinically in human populations. Mouse cancer cell lines allow researchers to study the influence of various genomic tumor profiles on clinical treatment outcomes. This is advantageous over orthotopic models, which are limited with regard to availability. BLI, combined with high-resolution measurement of tumor volume, contrast-enhanced micro-CT, and pathological analysis to evaluate *in situ* tumor growth, provides a reasonable model for longitudinal research on cancer biology and testing treatment effectiveness. A deeper evaluation of microenvironmental parameters throughout the whole body will aid in future characterization of these preclinical models.

## Acknowledgments

*Funding:* This work was supported by the Tianjin Municipal Education Commission Research Program (No. 2020KJ143) and funded by Tianjin Key Medical Discipline (Specialty) Construction Project (No. TJYXZDXK-009A).

## Footnote

*Reporting Checklist:* The authors have completed the ARRIVE reporting checklist. Available at https://tcr.amegroups.com/article/view/10.21037/tcr-23-522/rc

*Data Sharing Statement:* Available at https://tcr.amegroups.com/article/view/10.21037/tcr-23-522/dss

*Peer Review File:* Available at https://tcr.amegroups.com/article/view/10.21037/tcr-23-522/prf

*Conflicts of Interest:* All authors have completed the ICMJE uniform disclosure form (available at https://tcr.amegroups.com/article/view/10.21037/tcr-23-522/coif). The authors have no conflicts of interest to declare.

*Ethical Statement:* The authors are accountable for all aspects of the work in ensuring that questions related to the accuracy or integrity of any part of the work are appropriately investigated and resolved. All experiments were conducted according to local institutional guidelines and approved by the Animal Care and Use Committee of Tianjin Medical University Cancer Institute & Hospital, Tianjin, China (Animal Protocol No. 2022035).



## References

1. Biller LH, Schrag D. Diagnosis and Treatment of Metastatic Colorectal Cancer: A Review. JAMA 2021;325:669-85.
2. Li S, Liu J, Zheng X, et al. Tumorigenic bacteria in colorectal cancer: mechanisms and treatments. Cancer Biol Med 2021. [Epub ahead of print]. doi: 10.20892/

 

j.issn.2095-3941.2020.0651.
3. Montalban-Arques A, Scharl M. Intestinal microbiota and colorectal carcinoma: Implications for pathogenesis, diagnosis, and therapy. EBioMedicine 2019;48:648-55.
4. Zhu J, Long T, Gao L, et al. RPL21 interacts with LAMP3 to promote colorectal cancer invasion and metastasis by regulating focal adhesion formation. Cell Mol Biol Lett 2023;28:31.
5. Di Nicolantonio F, Vitiello PP, Marsoni S, et al. Precision oncology in metastatic colorectal cancer - from biology to medicine. Nat Rev Clin Oncol 2021;18:506-25.
6. Gamez-Belmonte R, Mahapatro M, Erkert L, et al. Epithelial presenilin-1 drives colorectal tumour growth by controlling EGFR-COX2 signalling. Gut 2023;72:1155-66.
7. Neto Í, Rocha J, Gaspar MM, et al. Experimental Murine Models for Colorectal Cancer Research. Cancers (Basel) 2023;15:2570.
8. Liang W, Liu H, Zeng Z, et al. KRT17 Promotes T-lymphocyte Infiltration Through the YTHDF2-CXCL10 Axis in Colorectal Cancer. Cancer Immunol Res 2023;11:875-94.
9. Novellasdemunt L, Kucharska A, Baulies A, et al. USP7 inactivation suppresses APC-mutant intestinal hyperproliferation and tumor development. Stem Cell Reports 2023;18:570-84.
10. Bürtin F, Mullins CS, Linnebacher M. Mouse models of colorectal cancer: Past, present and future perspectives. World J Gastroenterol 2020;26:1394-426.
11. Armacki M, Polaschek S, Waldenmaier M, et al. Protein Kinase D1, Reduced in Human Pancreatic Tumors, Increases Secretion of Small Extracellular Vesicles From Cancer Cells That Promote Metastasis to Lung in Mice. Gastroenterology 2020;159:1019-1035.e22.
12. Rezapour S, Hosseinzadeh E, Marofi F, et al. Epigenetic-based therapy for colorectal cancer: Prospect and involved mechanisms. J Cell Physiol 2019;234:19366-83.
13. Gerstberger S, Jiang Q, Ganesh K. Metastasis. Cell 2023;186:1564-79.
14. Wirtz S, Popp V, Kindermann M, et al. Chemically induced mouse models of acute and chronic intestinal inflammation. Nat Protoc 2017;12:1295-309.
15. Doetschman T, Georgieva T. Gene Editing With CRISPR/Cas9 RNA-Directed Nuclease. Circ Res 2017;120:876-94.
16. Sánchez-Félix M, Burke M, Chen HH, et al. Predicting bioavailability of monoclonal antibodies after subcutaneous administration: Open innovation challenge. Adv Drug Deliv Rev 2020;167:66-77.
17. Mezzanotte L, van 't Root M, Karatas H, et al. In Vivo Molecular Bioluminescence Imaging: New Tools and Applications. Trends Biotechnol 2017;35:640-52.
18. Salunkhe S, Dheeraj, Basak M, et al. Surface functionalization of exosomes for target-specific delivery and in vivo imaging & tracking: Strategies and significance. J Control Release 2020;326:599-614.
19. Fleten KG, Bakke KM, Mælandsmo GM, et al. Use of non-invasive imaging to monitor response to aflibercept treatment in murine models of colorectal cancer liver metastases. Clin Exp Metastasis 2017;34:51-62.
20. Alsawaftah N, Farooq A, Dhou S, et al. Bioluminescence Imaging Applications in Cancer: A Comprehensive Review. IEEE Rev Biomed Eng 2021;14:307-26.
21. Gómez-Cuadrado L, Tracey N, Ma R, et al. Mouse models of metastasis: progress and prospects. Dis Model Mech 2017;10:1061-74.
22. Chen RX, Chen X, Xia LP, et al. N(6)-methyladenosine modification of circNSUN2 facilitates cytoplasmic export and stabilizes HMGA2 to promote colorectal liver metastasis. Nat Commun 2019;10:4695.
23. Dong, S., Liang, S., Cheng, Z. et al. ROS/PI3K/Akt and Wnt/β-catenin signalings activate HIF-1α-induced metabolic reprogramming to impart 5-fluorouracil resistance in colorectal cancer. J Exp Clin Cancer Res 2022;41:15.
24. Dorning A, Dhami P, Panir K, et al. Bioluminescent imaging in induced mouse models of endometriosis reveals differences in four model variations. Dis Model Mech 2021;14:dmm049070.
25. Jenkins DE, Oei Y, Hornig YS, et al. Bioluminescent imaging (BLI) to improve and refine traditional murine models of tumor growth and metastasis. Clin Exp Metastasis 2003;20:733-44.
26. Villa A, Garofalo M, Crescenti D, et al. Transplantation of autologous extracellular vesicles for cancer-specific targeting. Theranostics 2021;11:2034-47.
27. Iwano S, Sugiyama M, Hama H, et al. Single-cell bioluminescence imaging of deep tissue in freely moving animals. Science 2018;359:935-9.
28. Tanino R, Amano Y, Tong X, et al. Anticancer Activity of ZnO Nanoparticles against Human Small-Cell Lung Cancer in an Orthotopic Mouse Model. Mol Cancer Ther 2020;19:502-12.
29. Jarry U, Bostoën M, Pineau R, et al. Orthotopic model of lung cancer: isolation of bone micro-metastases after tumor escape from Osimertinib treatment. BMC Cancer

 

2021;21:530.
30. Gonzalvez F, Vincent S, Baker TE, et al. Mobocertinib (TAK-788): A Targeted Inhibitor of EGFR Exon 20 Insertion Mutants in Non-Small Cell Lung Cancer. Cancer Discov 2021;11:1672-87.
31. Hassell BA, Goyal G, Lee E, et al. Human Organ Chip Models Recapitulate Orthotopic Lung Cancer Growth, Therapeutic Responses, and Tumor Dormancy In Vitro. Cell Rep 2017;21:508-16.
32. Guerra C, Barbacid M. Genetically engineered mouse models of pancreatic adenocarcinoma. Mol Oncol 2013;7:232-47.
33. Kersten K, de Visser KE, van Miltenburg MH, et al. Genetically engineered mouse models in oncology research and cancer medicine. EMBO Mol Med 2017;9:137-53.
34. Zhu X, Wang F, Wu X, et al. FBX8 promotes metastatic dormancy of colorectal cancer in liver. Cell Death Dis 2020;11:622.
35. Fujinami Y, Inoue S, Ono Y, et al. Sepsis Induces Physical and Mental Impairments in a Mouse Model of Post-Intensive Care Syndrome. J Clin Med 2021;10:1593.
36. Zhang HF, Zhang HB, Wu XP, et al. Fisetin alleviates sepsis-induced multiple organ dysfunction in mice via inhibiting p38 MAPK/MK2 signaling. Acta Pharmacol Sin 2020;41:1348-56.
37. Chen Y, Keskin D, Sugimoto H, et al. Podoplanin+ tumor lymphatics are rate limiting for breast cancer metastasis. PLoS Biol 2018;16:e2005907.
38. Kim KW, Jeong JU, Lee KH, et al. Combined NK Cell Therapy and Radiation Therapy Exhibit Long-Term Therapeutic and Antimetastatic Effects in a Human Triple Negative Breast Cancer Model. Int J Radiat Oncol Biol Phys 2020;108:115-25.
39. Han, Y.H., J.G. Mun, H.D. Jeon, et al. Betulin Inhibits Lung Metastasis by Inducing Cell Cycle Arrest, Autophagy, and Apoptosis of Metastatic Colorectal Cancer Cells. Nutrients 2019;12:E66.
40. Redente EF, Black BP, Backos DS, et al. Persistent, Progressive Pulmonary Fibrosis and Epithelial Remodeling in Mice. Am J Respir Cell Mol Biol 2021;64:669-76.
41. Hu HT, Wang Z, Kim MJ, et al. The Establishment of a Fast and Safe Orthotopic Colon Cancer Model Using a Tissue Adhesive Technique. Cancer Res Treat 2021;53:733-43.

**Cite this article as:** Song WJ, Zhang F, Wang ZY, Wang ZS, Wang BY, Jia JR. Colorectal cancer mouse metastasis model combining bioluminescent and micro-computed tomography imaging for monitoring the effects of 5-fluorouracil treatment. Transl Cancer Res 2023;12(10):2572-2581. doi: 10.21037/tcr-23-522

 